Dyes and Pigments 99 (2013) 520–525

Contents lists available at SciVerse ScienceDirect

Dyes and Pigments

journal homepage: www.elsevier.com/locate/dyepig

Short communication

Deep blue fluorescent 2,5-bis(phenylsilyl)-substituted 3,4-diphenylsiloles: Synthesis, structure and aggregation-induced emission

Jian Zhou[a], Bairong He[a], Bin Chen[a], Ping Lu[c], Herman H.Y. Sung[b], Ian D. Williams[b], Anjun Qin[d], Huayu Qiu[a], Zujin Zhao[a,*], Ben Zhong Tang[b,**]

[a] College of Material, Chemistry and Chemical Engineering, Hangzhou Normal University, Hangzhou 310036, China
[b] Department of Chemistry, Institute for Advanced Study, State Key Laboratory of Molecular Neuroscience and Institute of Molecular Functional Materials, The Hong Kong University of Science & Technology, Clear Water Bay, Kowloon, Hong Kong, China
[c] State Key Laboratory of Supramolecular Structure and Materials, Jilin University, Changchun 130012, China
[d] Department of Polymer Science and Engineering, Zhejiang University, Hangzhou 310027, China

A R T I C L E I N F O

Article history:
Received 18 April 2013
Received in revised form
11 May 2013
Accepted 17 May 2013
Available online 24 May 2013

Keywords:
Aggregation-induced emission
Silole
Fluorescence
Crystallography
Blue chromophore
Organosilicon

A B S T R A C T

A series of 2,5-bis(phenylsilyl)-substituted 3,4-diphenylsiloles were synthesized by one pot reaction in moderate yields (47–66%) and characterized by NMR, Mass and elemental analysis. Their crystals were grown from THF/methanol mixtures and analyzed by single-crystal X-ray diffraction. The electronic structures and energy levels were calculated by B3LYP/6-31G(d) basis set. The results show that these new siloles possess a flexible conformation with novel $\sigma-\pi^*$ conjugation. The absorption and fluorescence spectra were measured in the solution and aggregate states. Whereas they are weakly fluorescent in solutions, they are induced to emit strong deep blue light in solid films and crystals, demonstrating an aggregation-induced emission (AIE) characteristic.

1. Introduction

In 2001, a novel phenomenon of aggregation-induced emission (AIE) [1] was found by Tang's group, from propeller-like siloles, such as 1-methyl-1,2,3,4,5-pentaphenylsilole (MPPS) and 1,1,2,3,4,5-hexaphenylsilole (HPS). These silole molecules show faint fluorescence in solutions, but are induced to emit intensely with the aggregate formation. This interesting AIE phenomenon is opposite to aggregation-caused emission quenching effect widely observed from conventional chromophores, and has drawn intense research interest due to its bright prospect in materials science and biotechnology. To have a deep insight into the AIE phenomenon, systematic theoretical and experimental researches were carried out. The results disclose that the AIE effect of propeller-like siloles is mainly caused by the restriction of intramolecular rotations of the phenyl rotors against the silole ring stator [1c,2,3a]. The presence of the phenyl rings at the 3,4-positions is crucial. Without them, the phenyl rings at the 2,5-positions become coplanar with the central silole ring, leading to a better conjugation and more rigid conformation. Therefore, the emission efficiency in solutions is improved and the AIE characteristic disappears [1c]. The emission color of siloles is controlled largely by the conjugation extended through the 2,5-positions of silole ring, as well as electronic and steric structures of substituents at both positions [3–5].

Recently, blue luminescent materials are highly pursued [6], for they are essential for high quality full color displays and white lightening. Based on AIE motif, many efficient solid-state blue emitters have been developed [7]. However, to the best of our knowledge, almost all the AIE-active siloles fluoresce in the green to red region [3–5]. And blue siloles, especially deep blue ones, are really infrequent. For instance, MPPS and HPS that carry two phenyl rings at the 2,5-positions only show green light (490–500 nm) in the solution and aggregate states. Replacing the phenyl rings with silylethynyl

---

* Corresponding author. Tel.: +86 571 28867898; fax: +86 571 28867899.
** Corresponding author.
E-mail addresses: zujinzhao@gmail.com (Z. Zhao), tangbenz@ust.hk (B.Z. Tang).

0143-7208/$ – see front matter © 2013 Elsevier Ltd. All rights reserved.
http://dx.doi.org/10.1016/j.dyepig.2013.05.016

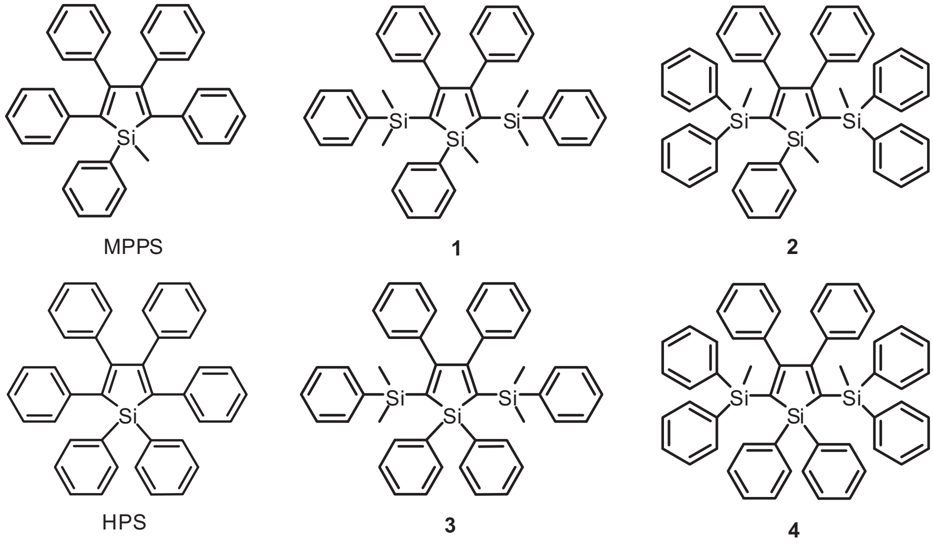

Fig. 1. Molecular structures of MPPS, HPS and 2,5-bis(phenylsilyl)-substituted 3,4-diphenylsiloles.

substituents can hardly move the emission to blue region neither [3a,b]. In order to obtain blue fluorescence, a series of tailored silole derivatives (Fig. 1) with flexible *sp*^{3} hybridized silicon linkages between silole core and phenyl rings at the 2,5-positions are rationally designed. It is envisioned that decreasing the conjugation between silole ring and aromatic substituents at the 2,5-positions may shift the emission wavelength into blue region. Another issue we concerned more is whether these silole derivatives are AIE-active still when no phenyl rotors are bonded directly at the 2,5-positions of the silole ring. Herein, we will present the synthesis and optical properties of these new silole derivatives.

2. Experimental

2.1. General

THF was distilled from sodium benzophenone ketyl under nitrogen immediately prior to use. Di(phenylethynyl)silanes (**5** and **6**) were prepared by lithiation of phenylacetylene followed by reaction with dichlorosilanes [4j]. All the chemicals and other reagents were purchased from Aldrich and used as received without further purification.

^{1}H and ^{13}C NMR spectra were measured on a Bruker AV 300 spectrometer in CD_2Cl_2 using tetramethylsilane (TMS; $\delta = 0$) as internal reference. UV spectra were measured on a Milton Roy Spectronic 3000 Array spectrophotometer. Photoluminescence (PL) spectra were recorded on a Perkin–Elmer LS 55 spectrofluorometer. The absolute PL quantum yields of solid films were measured according to the literature method [8] by a C-701 integrating sphere. The MALDI-TOF mass spectra were recorded on a GCT premier CAB048 mass spectrometer. Elemental analysis was performed on an Elementary Vario EL analyzer. Crystal X-ray diffraction intensity data were collected on a Bruker–Nonices Smart Apex CCD diffractometer with graphite monochromated Mo Kα radiation. Processing of the intensity data was carried out using the SAINT and SADABS routines, and the structure and refinement were conducted by the SHELTL suite of X-ray programs (version 6.10).

2.2. Preparation of nanoaggregates

Stock THF solutions of the luminogens with a concentration of 10^{-4} M were prepared. Aliquots of the stock solution were transferred to 10 mL volumetric flasks. After appropriate amounts of THF were added, water was added dropwise under vigorous stirring to furnish 10^{-5} M solutions with different water contents. The PL measurements of the resultant solutions were then performed immediately.

2.3. Synthesis

2.3.1. 2,5-Bis(dimethyl(phenyl)silyl)-1-methyl-1,3,4-triphenylsilole (**1**)

A solution of lithium naphthalenide (LiNaph) was prepared by stirring a mixture of naphthalene (2.56 g, 20 mmol) and lithium granular (0.14 g, 20 mmol) in dry THF (30 mL) for 4 h at room

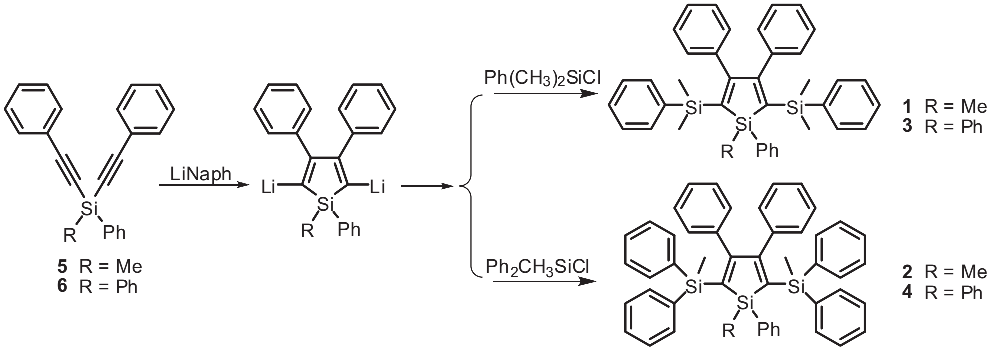

Scheme 1. Synthetic routes to siloles **1**–**4**.

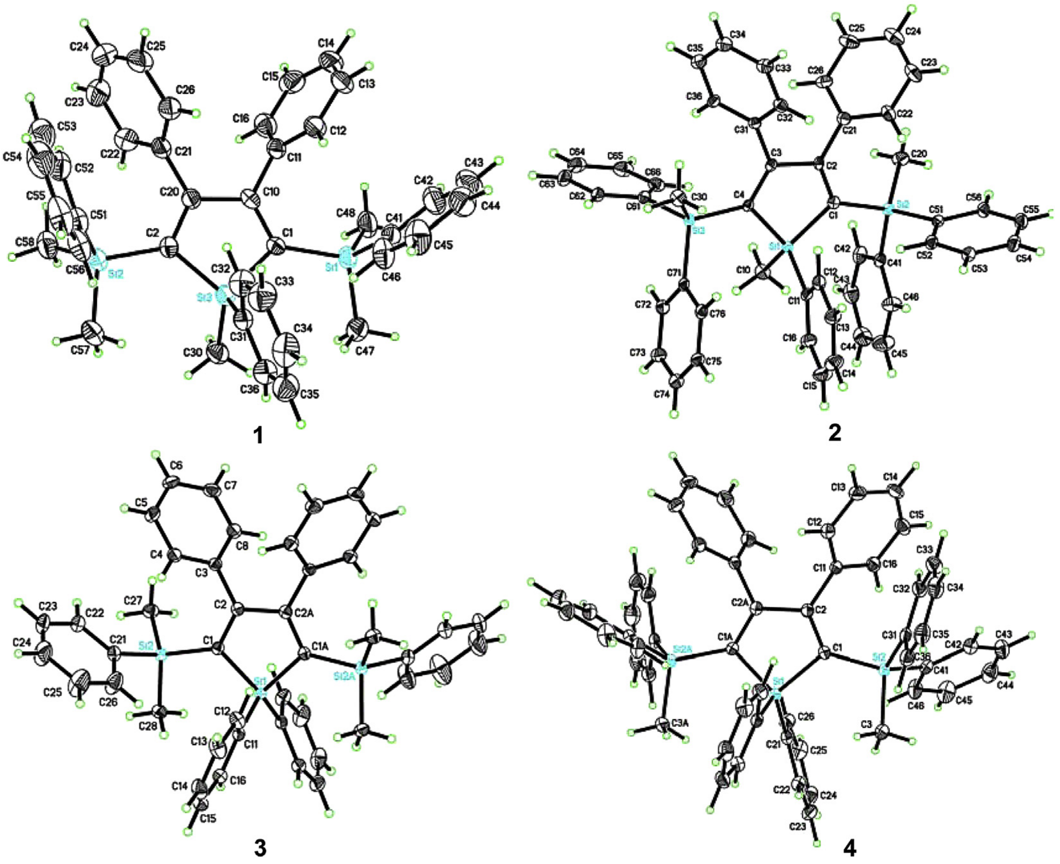

Fig. 2. ORTEP drawings of siloles **1** (CCDC 922983), **2** (CCDC 922984), **3** (CCDC 922985) and **4** (CCDC 922986).

temperature under nitrogen. Then a solution of methyl(phenyl)bis(phenylethynyl)silane (1.6 g, 5 mmol) in THF (10 mL) was added dropwise into the solution of LiNaph. After stirring for 30 min at room temperature, to the mixture was added dropwise $Ph(CH_3)_2SiCl$ (8 mL, 20 mmol). After stirring for 1 h at room temperature, the mixture was poured into water and extracted with dichloromethane twice. The combined organic layers were washed by water and then dried by magnesium sulfate. After filtration, the solvent was evaporated under reduced pressure, and then the residue was purified through column chromatography (silica gel, hexane as eluent) to afford **1** (2.0 g, 66% yield) as white solid. ^{1}H NMR (300 MHz, CD_2Cl_2), δ (TMS, ppm): 7.46–7.32 (m, 5H), 7.23–7.17 (m, 2H), 7.14–7.04 (m, 8H), 6.98–6.91 (m, 6H), 6.79–6.76 (m, 4H), 0.27 (s, 3H), −0.15 (s, 6H), −0.21 (s, 6H). ^{13}C NMR (75 MHz, CD_2Cl_2), δ (TMS, ppm): 172.0, 144.2, 143.1, 140.9, 135.1, 134.7, 134.6, 130.1, 129.6, 129.0, 128.6, 128.0, 127.6, 126.9, −0.4, −1.0, −6.1.

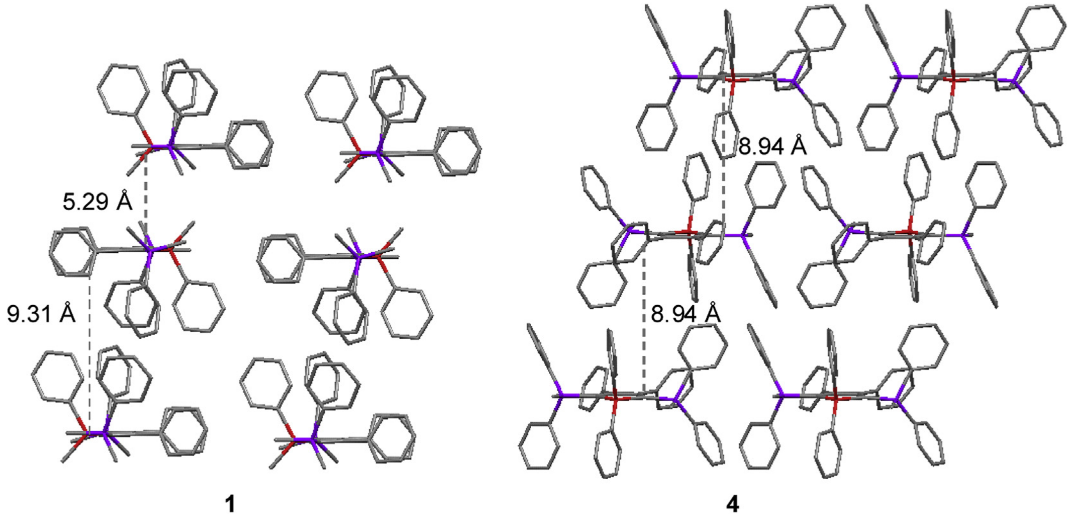

Fig. 3. Molecular packings of siloles **1** and **4** in crystals, with indicated distance between the parallel planes of silole rings. Hydrogen atoms are omitted for clarity.

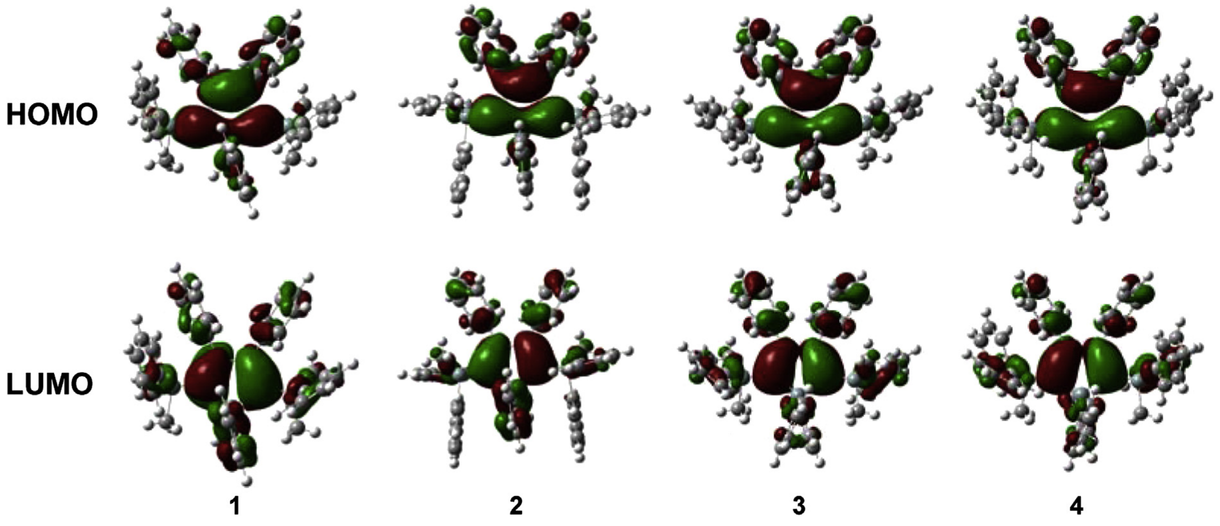

Fig. 4. Optimized molecular structures, and molecular orbital amplitude plots of HOMOs and LUMOs of siloles **1**–**4** calculated using B3LYP/6-31G(d) basis set.

MALDI-TOF-MS (*m*/*z*) calcd for $C_{39}H_{40}Si_3$: 592.2438 (M^+), found 615.1047 (M + Na^+). Anal. Calcd for $C_{39}H_{40}Si_3$: C, 78.99; H, 6.80. Found: C, 78.78; H, 6.84%.

2.3.2. *2,5-Bis(methyldiphenylsilyl)-1-methyl-1,3,4-triphenylsilole (**2**)*

The procedure was analogous to that described for **1** (59% yield, a white solid). ^{1}H NMR (300 MHz, $CDCl_3$), δ (TMS, ppm): 7.49–7.31 (m, 17H), 7.04–6.99 (m, 8H), 6.87–6.83 (m, 2H), 6.78–6.73 (m, 4H), 6.66–6.63 (m, 4H), −0.03 (s, 6H), −0.16 (s, 3H). ^{13}C NMR (75 MHz, $CDCl_3$), δ (TMS, ppm): 173.1, 143.4, 142.4, 138.8, 138.6, 135.6, 135.0, 133.7, 129.9, 129.4, 129.2, 129.1, 128.4, 128.0, 127.8, 127.4, 126.8, −2.4, −6.6. MALDI-TOF-MS (*m*/*z*) calcd for $C_{49}H_{44}Si_3$: 716.2751 (M^+), found 739.2454 (M + Na^+). Anal. Calcd for $C_{49}H_{44}Si_3$: C, 82.07; H, 6.18. Found: C, 81.88; H, 6.21%.

2.3.3. *2,5-Bis(dimethyl(phenyl)silyl)-1,1,3,4-tetraphenylsilole (**3**)*

The procedure was analogous to that described for **1**. White solid, 56% yield. ^{1}H NMR (300 MHz, CD_2Cl_2), δ (TMS, ppm): 7.76–7.73 (m, 4H), 7.53–7.39 (m, 6H), 7.15–7.09 (m, 2H), 7.00–6.86 (m, 10H), 6.81–6.78 (m, 4H), 6.69–6.66 (m, 4H), −0.18 (s, 12H). ^{13}C NMR (75 MHz, CD_2Cl_2), δ (TMS, ppm): 173.7, 143.5, 142.9, 140.8, 136.5, 134.5, 132.7, 130.7, 129.6, 128.8, 128.7, 127.8, 127.6, 126.9, −0.3. MALDI-TOF-MS (*m*/*z*) calcd for $C_{44}H_{42}Si_3$: 654.2594 (M^+), found 656.0916 (M + H^+), 678.2716 (M + Na^+). Anal. Calcd for $C_{44}H_{42}Si_3$: C, 80.68; H, 6.46. Found: C, 80.36; H, 6.45%.

2.3.4. *2,5-Bis(methyldiphenylsilyl)-1,1,3,4-tetraphenylsilole (**4**)*

The procedure was analogous to that described for **1** (47% yield, a white solid). ^{1}H NMR (300 MHz, CD_2Cl_2), δ (TMS, ppm): 7.46–7.41 (m, 6H), 7.33–7.28 (m, 4H), 7.17–7.12 (m, 4H), 7.01–6.90 (m, 16H), 6.86–6.81 (m, 2H), 6.74–6.69 (m, 4H), 6.60–6.57 (m, 4H), 0.02 (s, 6H). ^{13}C NMR (75 MHz, CD_2Cl_2), δ (TMS, ppm): 174.9, 142.6, 142.4, 138.3, 136.5, 135.7, 132.0, 130.5, 129.6, 129.1, 128.5, 127.8, 127.4, 126.8, −1.3. MALDI-TOF-MS (*m*/*z*) calcd for $C_{54}H_{46}Si_3$ 778.2907 (M^+), found 801.2826 (M + Na^+). Anal. Calcd for $C_{54}H_{46}Si_3$: C, 83.24; H, 5.95. Found: C, 83.16; H, 5.93%.

3. Results and discussion

Scheme 1 shows the synthetic routes to 2,5-bis(phenylsilyl)-substituted 3,4-biphenylsiloles. The detailed synthetic procedures and characterization data are given in Experimental section. Briefly, these new siloles are synthesized *via endo–endo* intramolecular reductive cyclization of di(phenylethynyl)silanes (**5** and **6**) in the

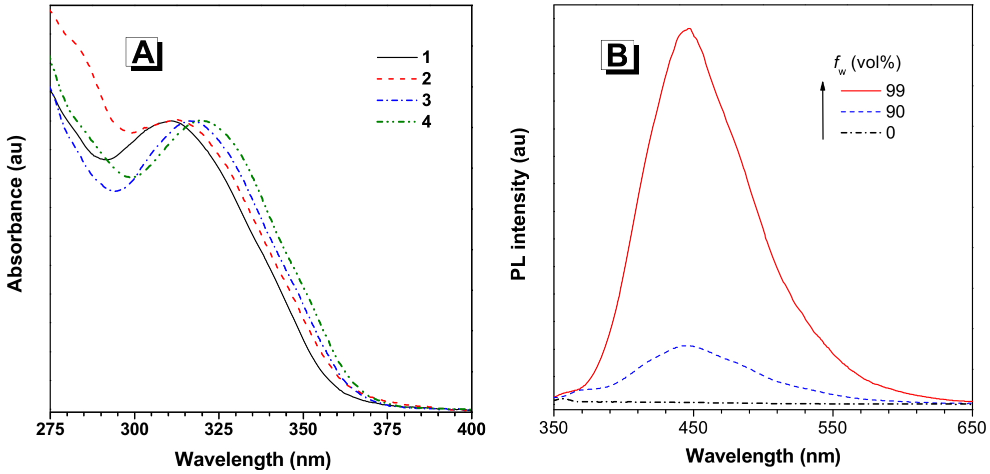

Fig. 5. (A) Absorption spectra of **1**–**4** in THF solutions. (B) PL spectra of **4** in THF/water mixtures with different water fraction (f_w), excited at 330 nm.

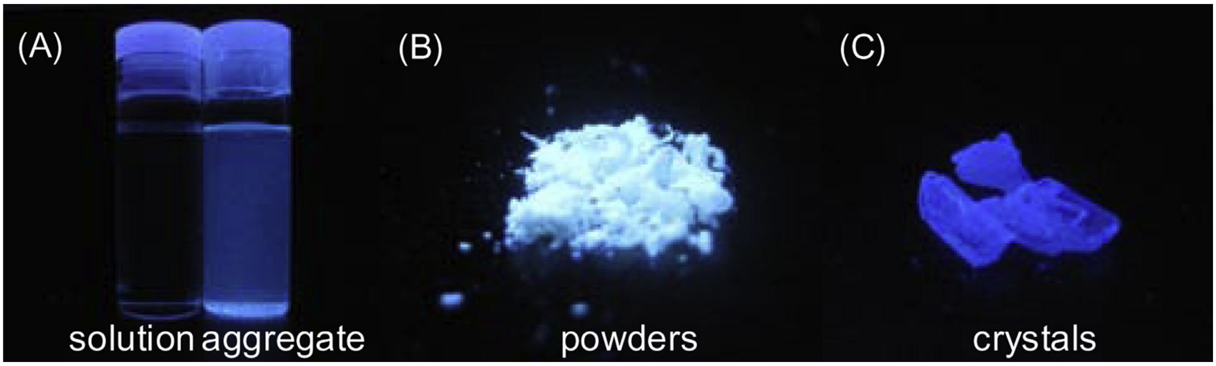

Fig. 6. Photos of (A) THF and aqueous solutions, (B) powders and (C) crystals of **4**, taken under the illumination of a UV lamp.

presence of LiNaph, followed by the treatment with diphenylmethylchlorosilane or phenyldimethylchlorosilane to afford target siloles (**1**–**4**) in moderate yields. These new siloles are soluble in common organic solvents such as dichloromethane and tetrahydrofuran (THF) but insoluble in water. The crystals of new siloles are grown from THF/methanol mixtures and are analyzed by single-crystal X-ray diffraction. The ORTEP plots of **1**–**4** are depicted in Fig. 2, where highly twisted conformations are observed for them. The molecular packings of siloles **1** and **4** in the crystalline state are displayed in Fig. 3 and those of **2** and **3** are given in Fig. S1 in Supporting Information (SI). It can be seen that the silole rings are located in a parallel pattern, but close π-stacking of silole rings is inhibited and π–π interactions between phenyl rings also greatly lowered, due to the propeller-like conformations. The theoretical calculations carried out using B3LYP/6-31G(d) basis set reveal that phenylsilyl substituents at the 2,5-positions have significant contributions to HOMOs and LUMOs (Fig. 4). Dense electronic cloud is located on the exocyclic Si–C bonds due to orbital overlapping between σ bonds on silicon and π* orbitals of butadiene fragment, leading to efficient σ–π* electronic delocalization [9].

Siloles **1**–**4** show similar absorption spectra in THF solutions (Fig. 5A). The absorption maxima of **3** and **4** are located at 318 and 320 nm, respectively, which are slightly red-shifted relative to those of **1** (311 nm) and **2** (313 nm), due to the inductive effect of phenyl rings at the 1,1-positions [4j,10]. In comparison with the absorption maxima of MPPS (363 nm) and HPS (366 nm), those of **1**–**4** have blue-shifted greatly by more than 46 nm, clearly demonstrating that the new silole molecules possess much less conjugation than MPPS and HPS. Siloles **1**–**4** show very weak emission in dilute THF solutions, only giving noisy signals but no discernable peaks. The fluorescence quantum yields (Φ_F) in solutions are measured below 0.01%, which are much lower than those of MPPS, HPS and other siloles [3–5].

To check whether siloles **1**–**4** are AIE active, water is added into their THF solutions and the PL spectra in THF/water mixtures are recorded. The PL spectra of **4** are illustrated in Fig. 5B as an example. It can be seen that an emission band appears and is boosted drastically when a large amount of water is added. Similar emission behaviors are also observed for **1**–**3** (Fig. S2), revealing that these new siloles are AIE active indeed. The aggregates of siloles **1**–**4** radiate intense deep blue light in the range of 444–447 nm, which are much bluer than those of MPPS (494 nm) and HPS (499 nm). Since water is a nonsolvent for these siloles, their molecules are aggregated in aqueous solutions. Thus, the intramolecular rotations, particularly those of phenyl rings at the 3,4-positions, are restricted due to the steric constraint in the aggregate state, which blocks the nonradiative relaxation and promotes radiative decay of the excited state, rendering the molecules emissive [1b,c].

Table 1
Optical properties of siloles **1**–**4**.

	λ_{abs} (nm)	λ_{em} (nm)			Φ_F (%)[d]
	Solution[a]	Crystal	Aggregate[b]	Film[c]	Film
1	311	420	447	448	18
2	313	421	444	442	21
3	318	413	446	445	12
4	320	416	447	444	16

[a] In THF solution (10 μM).
[b] Aggregate in aqueous solutions.
[c] Film drop-casted on quartz plate.
[d] Determined in amorphous film by integrating sphere. The Φ_F values in THF solutions are measured below 0.01%, using 9,10-diphenylanthracene as standard.

Efficient blue emissions are also observed from the crystals and films of siloles **1**–**4** (Fig. 6). Their crystals exhibit bluish-violet light in the range of 413–421 nm, while their films show deep blue emissions peaked at 442–448 nm (Fig. S3), which are quite close to those of the aggregates in aqueous solutions as compared in Table 1. The red-shifted emission of films relative to crystals, which is often observed from AIE luminogens [7b], is ascribed to the more planar molecular conformations in the amorphous films as well as intermolecular interactions induced thereby. The emissions of siloles **1**–**4** in films have blue-shifted by more than 50 nm in comparison with those of HPS, MPPS and 2,5-silylethynyl substituted siloles [3a,b], due to the weak σ–π* conjugation. The Φ_F values of siloles **1**–**4** in films are 18, 21, 12 and 16%, respectively, which are much higher than those in solutions, again confirming their AIE characteristics. These results demonstrate that the AIE characteristic is retained then if the there are no phenyl rotors conjugated directly to the 2,5-positions of the silole ring. Solid-state deep blue emissive siloles are achieved when sp^3 hybridized silyl substituents take the place of aromatic groups at the 2,5-positions of silole ring.

4. Conclusions

In summary, for the sake of creation of luminescent materials with excellent blue emission in the aggregate state, a new synthetic protocol is proposed, based on which a series of novel 2,5-bis(phenylsilyl)-substituted 3,4-diphenylsiloles are synthesized and characterized. Their crystal and electronic structures and photophysical properties are investigated. These new siloles show AIE characteristics even if the phenyl rings are not directly bonded to the 2,5-positions of silole ring, indicating that the phenyl rotors at the 3,4-positions are much more important to keep the AIE characteristic of siloles. Deep blue emissions are observed from these new siloles in the film and crystal states. The weak σ–π* conjugation between phenylsilyl groups and silole ring enables the molecule to emit much bluer lights than most siloles reported so far.

Acknowledgments

We acknowledge the financial support from the National Natural Science Foundation of China (51273053, 21104012 and 21074028), the National Basic Research Program of China (973 Program, 2013CB834702), the Natural Science Foundation of Zhejiang Province (Y4110331), the Program for Changjiang Scholars and Innovative Research Teams in Chinese Universities (IRT 1231) and the Project of Zhejiang Key Scientific and Technological Innovation Team (2010R50017). B. Z. Tang thanks the support of the Guangdong Innovative Research Team Program of China (20110C0105067115).

Appendix A. Supplementary data

Supplementary data related to this article can be found at http://dx.doi.org/10.1016/j.dyepig.2013.05.016.

References

[1] (a) Luo J, Xie Z, Lam JWY, Cheng L, Chen H, Qiu C, et al. Aggregation-induced emission of 1-methyl-1,2,3,4,5-pentaphenylsilole. Chemical Communications 2001:1740–1;
(b) Hong Y, Lam JWY, Tang BZ. Aggregation-induced emission: phenomenon, mechanism and applications. Chemical Communications 2009:4332–53;
(c) Hong Y, Lam JWY, Tang BZ. Aggregation-induced emission. Chemical Society Reviews 2011;40(11):5361–88.

[2] (a) Li Z, Dong Y, Mi B, Tang Y, Häussler M, Tong H, et al. Structural control of the photoluminescence of silole regioisomers and their utility as sensitive regiodiscriminating chemosensors and efficient electroluminescent materials. The Journal of Physical Chemstry B 2005;109(20):10061–6;
(b) Liu J, Su H, Meng L, Zhao Y, Deng C, Ng JCY, et al. What makes efficient circularly polarised luminescence in the condensed phase: aggregation-induced circular dichroism and light emission. Chemical Science 2012;3(9):2737–47.

[3] (a) Zhao Z, Wang Z, Lu P, Chan CYK, Liu D, Lam JWY, et al. Structural modulation of solid-state emission of 2,5-bis(trialkylsilylethynyl)-3,4-diphenylsiloles. Angewandte Chemie International Edition 2009;48(41):7608–11;
(b) Zhao Z, Liu D, Mahtab F, Xin L, Shen Z, Yu Y, et al. Synthesis, structure, aggregation-induced emission, self-assembly, and electron mobility of 2,5-bis(triphenylsilylethynyl)-3,4-diphenylsiloles. Chemistry–A European Journal 2011;17(21):5998–6008;
(c) Zhao Z, Chen S, Lam JWY, Jim CKW, Chan CYK, Wang Z, et al. Steric hindrance, electronic communication, and energy transfer in the photo- and electroluminescence processes of aggregation-induced emission luminogens. The Journal of Physical Chemistry C 2010;114(17):7963–72;
(d) Mei J, Wang J, Sun JZ, Zhao H, Yuan W, Deng C, et al. Siloles symmetrically substituted on their 2,5-positions with electron-accepting and donating moieties: facile synthesis, aggregation-enhanced emission, solvatochromism, and device application. Chemical Science 2012;3(2):549–58;
(e) Li Z, Dong Y, Lam JWY, Sun J, Qin A, Häußler M, et al. Functionalized siloles: versatile synthesis, aggregation-induced emission, and sensory and device applications. Advanced Functional Materials 2009;19(6):905–17.

[4] (a) Son HJ, Han WS, Chun JY, Lee CJ, Han JI, Ko J, et al. Spiro-silacycloalkyl tetraphenylsiloles with a tunable exocyclic ring: preparation, characterization, and device application of 1,1′-silacycloalkyl-2,3,4,5-tetraphenylsiloles. Organometallics 2007;26(3):519–26;
(b) Jiang T, Jiang Y, Qin W, Chen S, Lu Y, Lam JWY, et al. Naphthalene-substituted 2,3,4,5-tetraphenylsiloles: synthesis, structure, aggregation-induced emission and efficient electroluminescence. Journal of Materials Chemistry 2012;22(38):20266–72;
(c) Du X, Wang ZY. Donor–acceptor type silole compounds with aggregation-induced deep-red emission enhancement: synthesis and application for significant intensification of near-infrared photoluminescence. Chemical Communications 2011;47(14):4276–8;
(d) Boydston AJ, Yin Y, Pagenkopf BL. Synthesis and electronic properties of donor–acceptor π-conjugated siloles. Journal of the American Chemical Society 2004;126(12):3724–5;
(e) Lee J, Liu QD, Bai DR, Kang Y, Tao Y, Wang S. 2,3,4,5-Tetrafunctionalized siloles: syntheses, structures, luminescence, and electroluminescence. Organometallics 2004;23(26):6205–13;
(f) Sanchez JC, DiPasquale AG, Rheingold AL, Trogler WC. Synthesis, luminescence properties, and explosives sensing with 1,1-tetraphenylsilole- and 1,1-silafluorene-vinylene polymers. Chemistry of Materials 2007;19(26):6459–70;
(g) Sartin MM, Boydston AJ, Pagenkopf BL, Bard AJ. Electrochemistry, spectroscopy, and electrogenerated chemiluminescence of silole-based chromophores. Journal of the American Chemical Society 2006;128(31):10163–70;
(h) Zhan X, Risko C, Amy F, Chan C, Zhao W, Barlow S, et al. Electron affinities of 1,1-diaryl-2,3,4,5-tetraphenylsiloles: direct measurements and comparison with experimental and theoretical estimates. Journal of the American Chemical Society 2005;127(25):9021–9;
(i) Sartin MM, Boydston AJ, Pagenkopf BL, Bard AJ. Synthesis and characterization of perfluoroaryl-substituted siloles and thiophenes: a series of electron-deficient blue light emitting materials. Chemistry of Materials 2006;18(14):3261–9;
(j) Yamaguchi S, Endo T, Uchida M, Izumizawa T, Furukawa K, Tamao K. Toward new materials for organic electroluminescent devices: synthesis, structures, and properties of a series of 2, 5-diaryl-3,4-diphenylsiloles. Chemistry–A European Journal 2000;6(9):1683–92.

[5] (a) Zhan X, Barlow S, Marder SR. Substituent effects on the electronic structure of siloles. Chemical Communications 2009:1948–55;
(b) Yamaguchi S, Tamao K, Yamaguchi S, Tamao K. Silole-containing σ- and π-conjugated compounds. Journal of the Chemical Society, Dalton Transitions 1998:3693–702;
(c) Fu H, Cheng Y. Electroluminescent and photovoltaic properties of silole-based materials. Current Organic Chemistry 2012;16(11):1423–46.

[6] (a) Li HC, Lin YP, Chou PT, Cheng YM, Liu RS. Color tuning and highly efficient blue emitters of finite diphenylamino-containing oligo(arylenevinylene) derivatives using fluoro substituents. Advanced Functional Materials 2007;17(4):520–30;
(b) Jiang Z, Liu Z, Yang C, Zhong C, Qin J, Yu G, et al. Multifunctional fluorene-based oligomers with novel spiro-annulated triarylamine: efficient, stable deep-blue electroluminescence, good hole injection, and transporting materials with very high T_g. Advanced Functional Materials 2009;19(24):3987–95;
(c) Shih PI, Chuang CY, Chien CH, Diau EWG, Shu CF. Highly efficient non-doped blue-light-emitting diodes based on an anthrancene derivative end-capped with tetraphenylethylene groups. Advanced Functional Materials 2007;17(16):3141–6;
(d) Tao ST, Peng ZK, Zhang XH, Wang PF, Lee CS, Lee ST. Highly efficient non-doped blue organic light-emitting diodes based on fluorene derivatives with high thermal stability. Advanced Functional Materials 2005;15(10):1716–21;
(e) Tonzola CJ, Kulkarni AP, Gifford AP, Kaminsky W, Jenekhe SA. Blue-light-emitting oligoquinolines: synthesis, properties, and high-efficiency blue-light-emitting diodes. Advanced Functional Materials 2007;17(6):863–74;
(f) Gao Z, Liu Y, Wang Z, Shen F, Liu H, Sun G, et al. High-efficiency violet-light-emitting materials based on phenanthro[9,10-*d*]imidazole. Chemistry–A European Journal 2013;19(8):2602–5.

[7] (a) Zhao Z, Lam JWY, Tang BZ. Tetraphenylethene: a versatile AIE building block for the construction of efficient luminescent materials for organic light-emitting diodes. Journal of Materials Chemistry 2012;22(45):23726–40;
(b) Zhao Z, Chen S, Shen X, Mahtab F, Yu Y, Lu P, et al. Aggregation-induced emission, self-assembly, and electroluminescence of 4,40-bis(1,2,2-triphenylvinyl)biphenyl. Chemical Communications 2010;46(5):686–8;
(c) Zhao Z, Chen S, Lam JWY, Lu P, Zhong Y, Wong KS, et al. Creation of highly efficient solid emitter by decorating pyrene core with AIE-active tetraphenylethene peripheries. Chemical Communications 2010;46(13):2221–3;
(d) Huang J, Yang X, Wang J, Zhong C, Wang L, Qin J, et al. New tetraphenylethene-based efficient blue luminophors: aggregation induced emission and partially controllable emitting color. Journal of Materials Chemistry 2012;22(6):2478–84.

[8] Kawamura Y, Sasabe H, Adachi C. Simple accurate system for measuring absolute photoluminescence quantum efficiency in organic solid-state thin films. Japanese Journal of Applied Physics 2004;43(11A):7729–30.

[9] Sanchez JC, Trogler WC. Hydrosilylation of diynes as a route to functional polymers delocalized through silicon. Macromolecular Chemistry and Physics 2008;209(15):1527–40.

[10] Yamaguchi S, Jin RZ, Tamao K. Modification of the electronic structure of silole by the substituents on the ring silicon. Journal of Organometallic Chemistry 1998;559(1–2):73–80.